Measurement of Effective Diffusivity from Effluent Concentration of a Flow Through Diffusion Cell

The overall effective diffusion coefficient for 3.3 mm extrudates of 5A Zeolite and CO_2/N_2 at 292°K and 142 kN/m^2 was measured in a continually purged, well mixed, constant volume diffusion cell. The change of CO_2 concentration in the effluent stream resulting from a step change in the influent stream was used with appropriate parameters in the analytical solution to calculate diffusion coefficients for the 0 to 0.1 vol. % and 0.1 to 1.0 vol. % CO_2 concentration ranges.

A. C. FROST

Union Carbide Corp.
Tarrytown, NY

SCOPE

Overall effective diffusion coefficients, or their subsidiary components, have been found from the dynamic response of a packed bed to either pulse or step inputs, as typified by Hashimoto and Smith (1973) and Masamune and Smith (1965), or from numerous other methods typified by Burghardt and Smith (1979), Villermaux and Matras (1973), Kelly and Fuller (1980), Ma and Lee (1976), and Kondis and Dranoff (1971). While almost all of these methods were capable of isolating the individual internal rate constants that made up the overall effective diffusion coefficient from the external rate constants, they either were mathematically complicated, required special sample preparation, or were not conducive to high temperature-pressure operation.

Ideally, a system should be able to operate over a wide range of conditions, be free of complicating external mass transfer resistances, and be described in relatively simple mathematical terms. These criteria might be met with a simple flow through diffusion cell if the transient weight pick-up were determined from the history of the effluent concentration, and if the mixing of the gas passing through the cell were sufficiently severe to insure a uniform concentration throughout the cell and a negligible bulk film resistance around each pellet.

This work covers the development of a cell designed so that the passing gas was well mixed and could flow freely around each pellet. The transient change in the effluent concentration was monitored as the gas feed was switched from one composition to another. This transient response was used with the appropriate mathematical model describing this system to calculate the overall effective diffusion coefficient for 3.3 mm extrudates of 5A Zeolite and CO_2/N_2 at 292°K and 142 kN/m^2 over the 0 to 0.1 vol. % CO_2 and 0.1 to 1.0 vol. % CO_2 concentration ranges. The ability of the mathematical model to take into account the effect of changes in sample size and flow rate was tested with runs having different values for these parameters. Furthermore, the bulk film mass transfer resistance was examined as a function of the gas throughput rate.

CONCLUSIONS AND SIGNIFICANCE

The diffusion coefficient measured over the 0.1 to 1.0 vol. % CO_2 concentration range was uninfluenced by changes in the purge gas flow rate or the number of extrudates in the cell. Consequently, the analytical solution, which did not account for a bulk film mass transfer resistance, was satisfactory under these conditions. Furthermore, the measured overall effective diffusion coefficient for the 3.3 mm extrudates of 5A Zeolite was found to be influenced by macropore as well as micropore diffusion.

The diffusion coefficient measured over the 0 to 0.1 vol. % CO_2 concentration range increased with increasing flow rate, an indication that in this concentration range the bulk film mass transfer resistance was significant. Under these conditions the true diffusion coefficient was found from the extrapolation of a correlation of the measured diffusion coefficients with their corresponding flow rates.

These conclusions are significant in that they show a simple procedure has been developed which can rapidly measure overall effective diffusion coefficients over a wide range of anticipated process conditions.

Most separation and catalytic reaction processes are defined by both equilibrium and rate considerations. The rate limiting steps are often restricted to gas and liquid transport occurring within solid particles. This phenomena usually involves at least two components and is often described with an overall effective diffusion coefficient. Many methods have been used to measure

0001-1541-81-1222-0813-$2.00.

these coefficients or their subsidiary components for binary gas systems.

These methods are typified by the following authors: Masamune and Smith (1965) and Hashimoto and Smith (1973) have described the use of the response of a step input and an impulse input, respectively, to a packed bed for obtaining the various internal and external mass transfer coefficients. Burghardt and Smith (1979) have described pulse-response methods for two modifications of the single pellet Wicke-Kallenbach (1941) cell. Kelly and Fuller (1980) have used response methods with six single-pellet diffusion cells, each having only one end open to a well-mixed, flow through vessel. Villermaux and Matras (1973) have used a response method for a well-mixed, flow-through vessel containing loosely packed catalyst pellets. Ma and Lee (1976) have used the transient curve of a well-mixed constant volume diffusion cell. Kondis and Dranoff (1971) have calculated the overall effective diffusion coefficient from the transient weight pick-up of a sample suspended in a microbalance and exposed to the binary gas stream.

Although the packed bed techniques are operatively simple and could be used over a wide range of temperatures and pressures, the conditions under which the overall effective diffusion coefficient can be readily delineated from the external rate constants is somewhat restrictive. While the simpler diffusion cells which incorporate single, partially covered pellets circumvent the problems of external mass transfer effects, they require careful mounting of the pellets. Similarly, diffusion cells that are both free of external mass transfer effects and do not require special handling of the pellet samples are not always operable at high temperature and pressures, or they frequently must be used with cumbersome mathematical expressions.

The need for a screeming tool that could quickly and easily measure the overall effective diffusion coefficients and the equilibrium constants of a large number of adsorbents over a wide range of anticipated process conditions prompted the development of a well mixed, flow through diffusion cell that necessitated only minimal analysis of the step change of the inlet concentration. The initial testing runs described in this paper were made with 3.3 mm extrudates of commercial grade 5A Zeolite, LMS-5A ⅛ (Linde Molecular Sieve, 5A), and mixtures of 99.8+% pure CO_2 and cryogenic grade nitrogen.

MATHEMATICAL MODEL

The mathematical model assumes that the binary gas surrounding the particles within the diffusion cell is well mixed, that the inlet flow rate is constant, and that the particles have been uniformly equilibrated with a feed steam having a fixed initial composition. When a step change is made in this composition, the assumed equimolal, countercurrent diffusion that will then occur within spherical particles is described with an overall effective diffusion coefficient by

$$\frac{\partial C_A^*}{\partial t} = D\frac{\partial^2 C_A^*}{\partial r^2} + \frac{2D}{r}\frac{\partial C_A^*}{\partial r} \tag{1}$$

with the initial and boundary conditions inside the spheres being:

$$\text{At } t = 0 \quad C_A^*(r, 0) = C_{A0}^* \tag{2}$$

$$\text{At } r = 0 \text{ and } t > 0, \quad C_A^*(0, t) \text{ is finite} \tag{3}$$

When it is further assumed that the bulk film mass transfer resistance is negligible compared to the diffusional resistance within the sphere, the outside initial and boundary conditions are

$$\text{At } t = 0 \quad C_A(R, 0) = C_{A\text{in}} \tag{4}$$

$$-4\pi NR^2 D\left.\frac{\partial C_A^*}{\partial r}\right|_{r=R} = V\frac{\partial C_A}{\partial t} + F(C_A - C_{A\text{in}}) \tag{5}$$

Furthermore, the equilibrium relationship between the adsorbed and gas phase concentrations is assumed to be

$$C_A^* = C_A/K + S_1 \tag{6}$$

Use of the dummy variable $C_A' = C_A - C_{A\text{in}}$ with Eqs. 1-6 will result in a set of corresponding equations whose analogous heat transfer counterparts have been solved by Carslaw and Jaeger (1959). Substitution of the mass transfer constants for the heat transfer constants into their solution yields:

$$\frac{C_A - C_{A\text{in}}}{C_{A0} - C_{A\text{in}}} = 2\sum_{n=1}^{\infty}\frac{An\, e^{-\frac{DZ_n^2 t}{R^2}}}{A_n' + A_n'' - A_n'''} \tag{7}$$

with

$$A_n = FK/4\pi NRD - VKZ_n^2/4\pi NR^3 \tag{8}$$

$$A_n' = [VKZ_n^2/4\pi NR^3]^2 \tag{9}$$

$$A_n'' = Z_n^2[1 + 3VK/4N\pi R^3 - (2)(VK)(FK)/(4\pi NR^2D)^2] \tag{10}$$

$$A_n''' = [FK/4N\pi RD][1 - FK/4\pi NRD] \tag{11}$$

$$Z_n = (1 - A_n)TAN\, Z_n \tag{12}$$

A similar derivation can be made for cylindrical pellets if end effects are neglected. In this case substitution of mass transfer constants into the analogous heat transfer solution (Carslaw and Jaeger, 1959) yields:

$$\frac{C_A - C_{A\text{in}}}{C_{A0} - C_{A\text{in}}} = 2\sum_{n=1}^{\infty}\frac{B_n J_0(Z_n) e^{-\frac{DZ_n^2}{R^2}t}}{B_n' J_0(Z_n) + B_n''} \tag{13}$$

with

$$B_n = FK/2\pi NLD - VKZ_n^2/2\pi NR^2L \tag{14}$$

$$B_n' = [VK/\pi NR^2L + 1]Z_n^2 \tag{15}$$

$$B_n'' = [FK/2\pi NLD - VKZ_n^2/2\pi NR^2D]^2 \tag{16}$$

$$Z_n = A_n/J_1(Z_n) \tag{17}$$

In most situations the second and succeeding terms on the right hand side of Eqs. 7 and 13 converge in a relatively short period of time. Then only the first term is significant. Further-

more, if the output of the analyzer used to measure C_A, C_{A0}, and C_{Ain} can be expressed as $C_A = S_1 + S_2(MV)$, then Eqs. 7 and 13 can be written as:

$$MV - MV_{in} = (S_3)(e^{-DZ_1^2 t/R^2}) \tag{18}$$

Thus, it can be seen that a plot of $ln\,(MV - MV_{in})$ versus time will soon converge to a straight line with a slope, m, equal to DZ_1^2/R^2. Substitution of $D = mR^2/Z_1^2$ into Eqs. 12 and 14 will then yield for spheres:

$$TAN\ Z_1 = \frac{Z_1}{(1 - FKZ_1^2/m4\pi NR^3) + \dfrac{VKZ_1^2}{4\pi NR^3}} \tag{19}$$

and for cylinders,

$$Z_1 J_1(Z_1) = \left(\frac{KZ_1^2}{2\pi NLR^2}\right)\left(\frac{F}{m} - V\right)J_0(Z_1) \tag{20}$$

Consequently, the value for the overall effective diffusion coefficient can be found by: (1) measuring m from the slope of the converged portion of the $ln\,(MV - MV_{in})$ versus time curve; (2) using this value of m and the other known constants of the system in Eqs. 19 or 20 to find by trial with the aid of tables (Carslaw and Jaeger, 1959) the only unknown, Z_1, and (3) using m and Z_1 in $D = mR_1^2/Z_1^2$ to calculate D.

PHYSICAL SYSTEM

The physical system was designed to meet the two major requirements of the mathematical model: A sharp step change of the inlet feed concentration and good gas mixing within the diffusion cell itself. Figure 1 shows that either purge nitrogen or one of two CO_2-nitrogen mixtures are fed in a step-wise manner via three-way valves through a rotameter, a preheat coil, the diffusion cell itself, a back-pressure regulator in parallel with a by-pass line, and a dry test meter. The preheat coil and diffusion cell are immersed in a constant temperature bath. The effluent stream is automatically sampled and analyzed every 100 seconds with a gas chromatograph (*Gow Mac* Model 550) equipped with an electronic integrator (*Spectra-Physics*, System 1) and an automatic sampling valve (*Carle* valve minder).

Figure 2 shows that the diffusion cell itself was an industrial filter (*Cuno*, Model 1B) fitted with a stack of ten wire screen trays within the confines of the 7.0 cm diameter, 7.0 cm long stainless steel filter element. The incoming gas passed through the stainless steel filter, into the section containing the tray-supported pellets, and out through the center of the cell. The transient behavior of the empty cell subjected to a step change in the feed concentration indicated that the degree of turbulence induced from the passage of the incoming feed through the stainless steel filter was sufficient for good mixing. However, the achievement of such mixing of the gas phase to satisfy this boundary condition did not necessarily mean that it was so vigorous that the bulk film mass transfer resistance was relatively unimportant, as was also assumed in the mathematical model. Whether or not that objective was obtained could only be answered with experimental data.

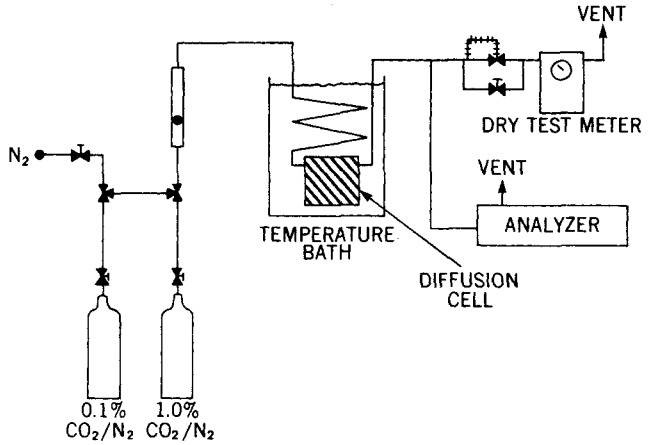

Figure 1. Schematic diagram of the flow through diffusion cell apparatus.

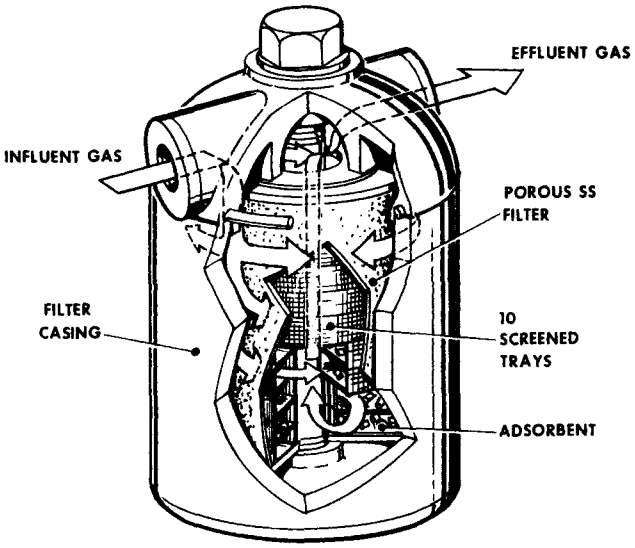

DIFFUSION CELL

Figure 2. Detail of the modified filter used for the flow through diffusion cell.

EXPERIMENTAL PROCEDURE

After the diffusion cell was loaded in a dry box with 51.3 grams of LMS 5A ⅛, activated at 653°K and 3.3 N/m², it was purged with nitrogen at the flow rate desired for the run. During this time the back-pressure regulator was adjusted to accommodate this flow at a 142 kN/m² cell pressure. When the run began, the nitrogen stream was changed to one that contained 0.1 vol. % CO_2/99.9 vol. % N_2 from one of the cylinders. When the CO_2 concentration in the effluent equaled that of the influent, a second run was begun with the substitution of the 0.1 vol. % CO_2 feed stream to one containing 1.0 vol. % CO_2. At the completion of this second run the bed was purged overnight with sufficient nitrogen to ensure complete removal of all adsorbed CO_2.

During the course of each of these runs the effluent stream was analyzed every 100 seconds. Furthermore, the absolute CO_2 concentrations and their MV_{in} values were obtained both before and after the two runs for each of the two feed cylinders. The temperature and pressure of the diffusion cell was maintained to within ±1°K and ±2 kN/m² of their respective set points. The measured flow rates were within 2% of their stated values.

As mentioned previously, the overall effective diffusion coefficient can be calculated from the slope of the $ln\,(MV_{in} - MV)$ versus time curve and Eq. 20, which contains the known constants of the system, including the slope, K, of the isotherm. The isotherm, in turn, can be constructed from material balances (In − Out = Amount Adsorbed) around the cell during each run. Since In − Out is directly proportional to $MV_{in} - MV$, the total amount of CO_2 adsorbed during a run is proportional to the integrated area under the $MV_{in} - MV$ vs. time curve. The area under the beginning part of this curve can be integrated graphically; the area under the later part of the curve can be integrated analytically to $t = \infty$, since it has been shown from Eq. 18 that during this part of the run the curve is described by a single exponential term. The

constants of this exponential term can be obtained from the $\ln (MV_{in} - MV)$ versus time curve.

The CO_2 equilibrium loadings were calculated in this manner each time the effective diffusivity was measured over a particular concentration range at a sufficiently low flow rate to yield a reasonably precise integrated $MV_{in} - MV$ vs. time curve. For instance, the CO_2 equilibrium loading of the LMS-5A for a 0.1 vol. % CO_2 concentration feed stream was found from a material balance around the cell at the end of the run, after the CO_2 feed concentration had been suddenly increased from 0 to 0.1 vol. %, and the LMS-5A had equilibrated to the 0.1 vol. % concentration level. Similarly, an additional loading was obtained in the same manner at the end of a sequential run, after the CO_2 feed concentration had again been suddenly increased from 0.1 to 1.0 vol. %, and the LMS-5A had equilibrated to the 1.0 vol. % concentration level. The total equilibrium loading for the 1.0 vol. % concentration was then obtained by adding the two equilibrium loadings found from the two runs made over the two intermediate concentration ranges.

EXPERIMENTAL RESULTS

The CO_2 equilibrium loadings calculated in this manner were plotted on semi-log paper against their corresponding CO_2 feed concentrations. The resulting curve was reasonably linear, as was expected for this type of Langmuirian system, and was in good agreement with other, independent data. Figure 3 shows this smoothed curve replotted on linear coordinates with the individual data points obtained during these runs. Values for K were obtained from Figure 3 by taking the inverse slope ($K = \Delta C_A/\Delta C$) of the lines representing average chords for those two portions of the isotherm covering the C_A ranges of 0 to 0.58×10^{-7} (0.1 vol. % CO_2) and 0.58 to 5.8×10^{-7} (1.0 vol. % CO_2). These K values are average values over these ranges. A closer match between the curve and the corresponding chord occurs when the runs are made over smaller concentration ranges, as was the case for the 0 to 0.1 vol. % CO_2 runs. Data taken in this manner will also minimize the effects of concentration and heat of adsorption on the measured diffusion coefficient. Thus, if the diffusion coefficient is desired for a given concentration, it should ideally be measured over a small range at that concentration.

Figures 4 and 5 show representative $\ln (MV_{in} - MV)$ versus time plots for the runs made over the 0-0.1 vol. % CO_2 and 0.1 – 1.0 vol.% CO_2 concentration ranges, respectively. The slopes of these curves were not only used to find the overall effective diffusion coefficient with the aid of $m = DZ_1^2/R^2$ and Eq. 20, but they were also used, for the low flow rate runs, to obtain the uptake of the adsorbent from the time of convergence to $t \rightarrow \infty$ by providing the exponential term required for the analytical integration of Equation 18. As stated previously, the uptake of the adsorbent from $t = 0$ to the time of convergence was calculated by the graphical integration of a separately plotted $MV_{in} - MV$ vs. time curve.

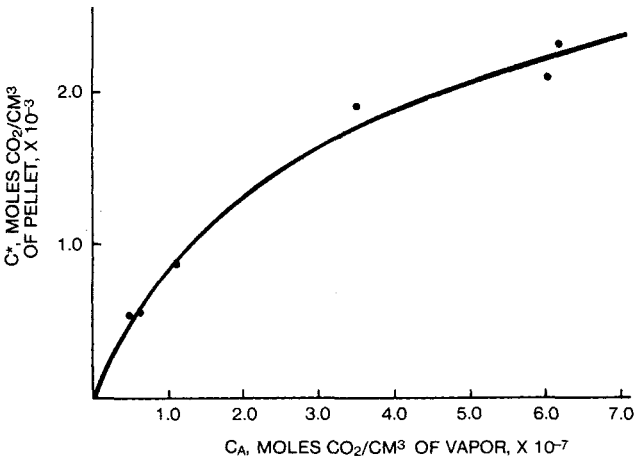

Figure 3. Equilibrium CO_2 isotherm with LMS-5A ⅛ at 292°K and 142 kN/m². Data points were calculated from the material balances taken around the cell during the course of the runs made with different feed gas concentrations.

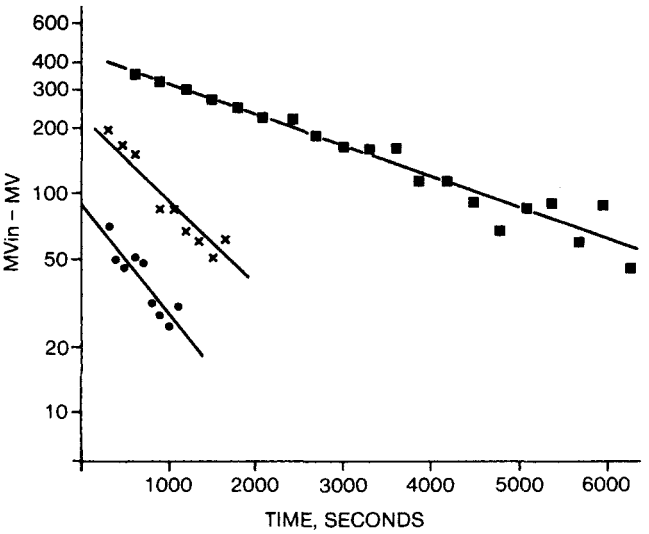

Figure 4. Effluent concentration curves for 292°K, 142 kN/m² runs of varying LMS-5A ⅛ adsorbent sample size and flow rate over the 0 to 0.1 vol. % CO_2 concentration range. ■ – 25.0 g, 261 cm³/s, $m = 3.22 \times 10^{-4}$ s⁻¹, $Z_1 = 2.01$, $D = 2.1 \times 10^{-6}$ cm²/s; X – 51.3 g, 2346 cm³/s, $m = 9.00 \times 10^{-4}$ s⁻¹, $Z_1 = 2.16$, $D = 5.1 \times 10^{-6}$ cm²/s; ● – 51.3 g, 3965 cm³/s, $m = 11.68 \times 10^{-4}$ s⁻¹, $Z_1 = 2.22$, $D = 6.2 \times 10^{-4}$ s⁻¹.

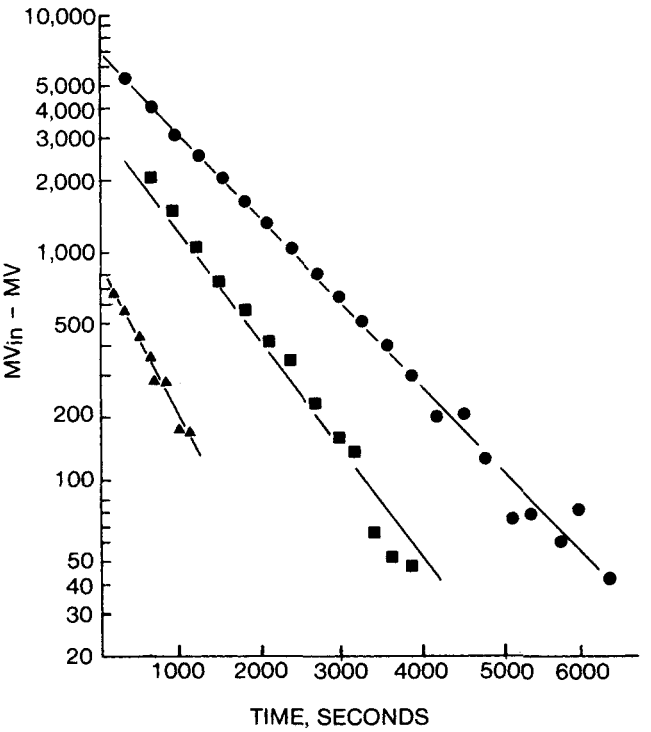

Figure 5. Effluent concentration curves for 292°K, 142 kN/m² runs of varying LMS-5A ⅛ adsorbent sample size and flow rate over the 0.1 to 1.0 vol. % CO_2 concentration range. ● – 51.3 g, 261 cm³/s, $m = 7.83 \times 10^{-4}$ s⁻¹, $Z_1 = 1.70$, $D = 7.2 \times 10^{-6}$ cm²/s; ■ – 25.0 g, 261 cm³/s, $m = 10.23 \times 10^{-4}$ s⁻¹, $Z_1 = 2.02$, $D = 6.7 \times 10^{-6}$ cm²/s; ▲ – 51.3 g, 3965 cm³/s, $m = 14.76 \times 10^{-4}$ s⁻¹, $Z_1 = 2.33$, $D = 7.2 \times 10^{-6}$ cm²/s.

The least mean square plots of Figures 4 and 5 indicated that the scatter in the points became pronounced when $MV_{in} - MV$ dropped below 100. Consequently, these points were given less weight when there were a larger number of other points having greater $MV_{in} - MV$ values, such as those shown for the middle run in Figure 5.

It can be seen that the most cumbersome part of the above-described experimental procedure involved the subsidiary determination of the isotherm. In many adsorbent screening tests the isotherm, and hence K, will already be known, so that only the readily measured m will be required to obtain the overall diffusion coefficient.

EFFECTS OF CHANGES IN PELLET CHARGE OR FLOW RATE

If the mathematical model describes the physical system accurately, it should correct for changes made in any of the operating parameters. Consequently, the same diffusion coefficient should be obtained regardless of the flow rate or the number of pellets present in the cell. This must mean that changes in these variables should effect both m and Z_1^2 in a compensating manner, so that the diffusion coefficient calculated from $D = mR_1^2/Z_1^2$ will remain the same.

Fewer pellets can be expected to remove less CO_2 from the gas as it passes through the cell, so that the difference between the inlet and outlet concentrations, i.e., $MV_{in} - MV$ will generally be less. On the other hand, what CO_2 is removed from the gas enters the fewer pellets at a higher rate, since the CO_2 concentration driving force is greater. This causes the tablets to equilibrate faster, which in turn causes MV to approach MV_{in} faster. Thus, the $ln\,(MV_{in} - MV)$ vs. time curve shown in Figure 5 for a run made with 25.0 grams of pellets lies lower, and has a steeper slope than the corresponding curve for the run made with 51.3 grams of pellets, but at the same flow rate and over the same concentration range. The differences in these slopes are compensated by differences in the calculated values for Z_1, so that the two measured diffusion coefficients, 6.7×10^{-6} and 7.2×10^{-6} cm²/s are within experimental error to one another.

This same behavior is observed when the size of the pellet charge remains the same but the flow rate is increased. In this case the higher flow rate would mean a shorter gas residence time, so that less of the CO_2 would be removed from the incoming feed and $MV_{in} - MV$ would generally be smaller. On the other hand, the resulting higher gas phase CO_2 concentration at the higher flow rate would mean a higher CO_2 concentration driving force, and hence a higher rate of adsorption; consequently, MV would be expected to approach MV_{in} more rapidly, with a resulting increase in the steepness of m. A comparison of the top and bottom curves in Figure 5 shows the effects of a fifteen-fold increase in the flow rate for a 51.3 gram bed over the same 0.1 to 1.0 vol. % CO_2 concentration range. The higher flow rate curve was generally lower and had a steeper slope than the lower flow rate curve. However, the value for Z_1 is corresponding increased so that the calculated diffusion coefficient was 7.2×10^{-6} cm²/s for both runs.

Equation 17 indicates that Z_1 will approach 2.405 at infinitely high flow rates when the inlet and outlet concentrations become identical. This limiting value is the same as that found in the exponential term of the equation describing diffusion from a cylinder to an outside gas having a constant boundary condition (Crank, 1956).

BULK FILM RESISTANCE

While the diffusion coefficients measured over the 0.1 vol. % to 1.0 vol. % CO_2 concentration range were relatively insensitive to changes in F, this was not the case for runs made over the 0 to 0.1 vol. % CO_2 concentration range. The measured diffusion coefficient for these runs increased as F increased. This behavior would be expected if the bulk film mass transfer resistance were significant at these conditions, since a decrease in this resistance at higher flow rates would be reflected by a higher measured diffusion coefficient.

The fact that bulk film mass transfer resistance was significant over one concentration range and not over the other can be explained by both a higher overall diffusion coefficient at this low concentration range and, because of the steeper isotherm for this concentration range, the need for a greater molar flux to pass through the bulk film with the lower gas concentration driving force.

If the relationship between the true overall effective diffusion coefficient, the measured diffusion coefficient, and the bulk film mass transfer coefficient is expressed as:

$$\frac{1}{D} = \frac{1}{D_0} + \frac{S_4}{k} \tag{21}$$

and if k is comparable to that given by Dwivedi and Upadhyay (1977) for flows past cylinders at particle Reynolds numbers greater than 10 as:

$$k \cong (\text{Constant})\, F^{0.59} \tag{22}$$

then Eqs. 21 and 22 can be combined to yield:

$$\frac{1}{D} = \frac{1}{D_0} + \frac{S_5}{F^{0.59}} \tag{23}$$

Thus, a plot of $1/D$ vs. $1/F^{0.59}$ will yield $1/D_0$ at its intersect. Figure 6 shows the data plotted in this manner with $D_0 = 10.2 \times 10^{-6}$ cm²/s obtained for the 0 to 0.1 vol. % CO_2 concentration runs and $D_0 = 6.8 \times 10^{-6}$ cm²/s obtained for the 0.1 to 1.0 vol. % CO_2 concentration runs.

The precision for measuring the individual overall diffusion coefficient, D, with the flow through diffusion cell may be reflected by the 8% standard deviation measured for the three runs made over the 0.1 vol. % to 1.0 vol. % CO_2 concentration range at the three highest flow rates. The accuracy for determining the true overall diffusion coefficient, D_0, with the flow through diffusion cell and Eq. 23 needs to be more clearly defined with additional data.

MICRO/MACRO-PORE DIFFUSION

In order to determine the relative importance of macropore diffusion to the overall mass transport within the pellets, a single set of diffusion cell runs were made over the two CO_2 concentration ranges with 51.2 grams of 1.19-2.38 mm diameter particles, having the size distribution shown in Table and obtained from crushing the 3.3 mm diameter extrudates. The CO_2 uptake rates for the 51.2 grams of 1.19-2.38 mm particles over the two concentration ranges were faster than the corresponding CO_2 uptake rates for 51.2 grams of uncrushed extrudates. This difference between the two sets of CO_2 uptake rates indicates that macropore diffusion was a significant component of the overall mass transport rate within the 3.3 mm pellets. If the only mass transport rate were the micropore diffusion taking place within the individual 1-10μm diameter zeolite crystallites making up both the crushed and uncrushed pellets, there would have been no difference between the CO_2 uptake rates found for the two differently sized particles.

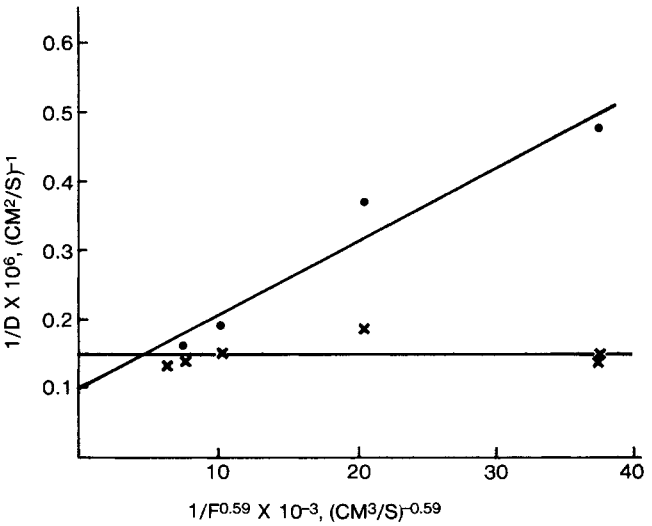

Figure 6. Effect of the bulk film mass transfer resistance on the measured diffusion coefficient. ● – runs made over the 0 to 0.1 vol. % CO_2 range. X – runs made over the 0.1 vol. % to 1.0 vol. % CO_2 range.

TABLE 1. SIZE DISTRIBUTION OF THE CRUSHED LMS-5A ⅛ EXTRUDATES

Particle Size, mm	% of Total Sample
3.36-2.38	0.3
2.38-2.00	38.1
2.00-1.68	25.7
1.68-1.41	21.0
1.41-1.19	12.8
1.19-1.00	0.1
Total	100.0

Although the CO_2 uptake rates were faster for the crushed pellets, the overall effective diffusion coefficients calculated from the slopes of the $ln\ (MV_{in} - MV)$ versus time curves and Eqs. 7 and 11 were only one fourth of the similarly calculated diffusion coefficients for the uncrushed pellets. Such a discrepancy could reflect the greater influence of the bulk film mass transfer resistance expected for smaller particles, or it could reflect an accidental movement of the smaller particles on the trays within the diffusion cell from a monolayer to a multilayer disposition. Additional runs would be required to explore these possibilities.

IMPROVING CELL PERFORMANCE

It is apparent that the diffusion cell described in this paper is so designed that it can operate over wide temperature and pressure ranges and yield an overall effective diffusion coefficient with minimal experimental and mathematical effort. Furthermore, the degree of induced mixing within the cell is sufficient to minimize the effect of the bulk film mass transfer resistance for many systems having the proper combination of particle size, effective diffusivity, and K.

The range of these parameters can be extended if the bulk film mass transfer coefficient is increased with the attainment of a greater degree of gas turbulence around each of the pellets. This could be done with the placement of a blower within the cell (Berty, 1974) or with a more sophisticated gas inlet system incorporating numerous small entrance jets (Villermauz and Matras, 1973). This last approach would permit the cell to maintain its advantage of being able to operate over wide temperature and pressure ranges.

ACKNOWLEDGMENT

The author wishes to thank Robert L. Webb, John M. Basile, and Dennis J. Cadden, of the Molecular Sieve Department, Linde Division, Union Carbide Corp., for their help in the construction and operation of the diffusion cell.

NOTATION

A_n, A'_n, A''_n, A'''_n = groupings of constants defined by Eqs. 8, 9, 10 and 11

B_n, B'_n, B''_n = groupings of constants defined by Eqs. 14, 15 and 16

C = concentration within gas stream, mol/cm^3

C^* = concentration within solid particle, mol/cm^3

C' = dummy variable, mol/cm^3

D_p = particle diameter, cm

D = measured diffusivity, cm^2/s

D_0 = extrapolated diffusivity to infinitely high flow rates, cm^2/s

F = flow rate through diffusion cell, cm^3/s

J_0, J_1 = Bessel functions of the first kind for the zero and first orders

K = slope of equilibrium isotherm

k = bulk film mass transfer coefficient, cm/s

L = length of cylindrical pellet, cm

MV = output of gas analyzer

m = absolute value of slope of exponential curve, s^{-1}

N = number of pellets in diffusion cell

R = outside radius of cylinder or sphere, cm

S_1, S_2, S_3, S_4, S_5 = constants

r = intermediate radius of cylinder or sphere, cm

t = time, s

V = volume of gas space in diffusion cell, cm^3

Z_n = variables defined by Eqs. 12 and 17

Subscripts

A = species A

A_0 = species A at time 0

in = incoming value

LITERATURE CITED

Berty, J. M., "Reactor For Vapor-Phase Catalytic Studies," *Chem. Eng. Prog.*, **70**, 78 (1974).

Burghardt, A., and J. M. Smith, "Dynamic Response of a Single Catalyst Pellet," *Chem. Eng. Sci.*, **34**, 267 (1979).

Carslaw, H. S., and J. C. Jaeger, *Conductor of Heat in Solids*, 2 ed., pp. 240-241, 329-330, Oxford at the Clarendon Press, Great Britain (1959).

Crank, J., *The Mathematics of Diffusion*, pp. 65-66, Oxford at the Clarendon Press, Great Britain (1956).

Dwivedi, P. N., and S. N. Upadhyay, "Particle-Fluid Mass Transfer in Fixed and Fluidized Beds," *Ind. Eng. Chem., Process Des. Dev.*, **16**, 157 (1977).

Hashimoto, N., and J. M. Smith, "Macropore Diffusion in Molecular Sieve Pellets By Chromatography," *Ind. Eng. Chem. Fund.*, **12**, 353 (1973).

Kelly, J. F., and O. M. Fuller, "An Evaluation of a Method for Investigation Sorption and Diffusion in Porous Solids," *Ind. Eng. Chem. Fund.*, **19**, 11 (1980).

Kondis, E. F., and J. S. Dranoff, "Kinetics of Ethane Sorption on 4A Molecular Sieve Crystal Powder and Pellets," Molecular Sieve Zeolites—II," *Adv. Chem. Ser. 102*, 171 (1971).

Masamune, S., and J. M. Smith, "Adsorption Rate Studies—Interaction of Diffusion and Surface Processes," *AIChE J.*, **11**, 34 (1971).

Ma, Y. H., and T. Y. Lee, "Transient Diffusion in Solids with a Bipore Distribution," *AIChE J.*, **22**, 147 (1976).

Villermaux, J., and J. Matras, "Une nouvelle formulation dynamique des interactions fluide solide—Application à des measures de diffusivités intraparticularies et de constantes d'equilibre d'adsorption," *Can. J. Chem. Eng.*, **51**, 636 (1973).

Wicke, E., and R. Kallenbach, "Surface Diffusion of Carbon Dioxide in Activated Charcoals," *Kolloid Z.*, **97**, 135 (1941).

Manuscript received March 5, 1979; revision received November 24, and accepted December 10, 1980.